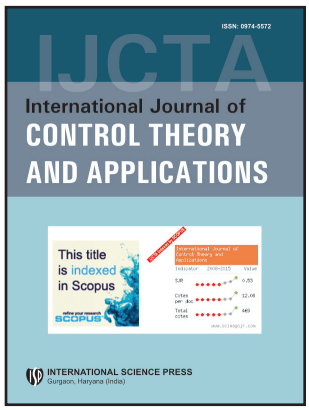

International Journal of Control Theory and Applications

ISSN : 0974-5572

Volume 10 • Number 16 • 2017

Determining Safe Electrical Zones for Placing Aircraft Navigation, Measurement and Microelectronic Systems in Static Thunderstorm Environment

P.R.P. Hoole[a], J. Fisher[b], K. Pirapaharan[c], Al Khalid Hj Othman[d], Norhuzaimin Julai[e], Aravind CV[f], K.S. Senthilkumar[g] and S.R.H. Hoole[h]

[a]*Corresponding author, Department of Electrical and Electronic Engineering, Universiti Malaysia Sarawak, Malaysia. Email: prphoole@gmail.com or prhoole@unimas.my*
[b,c]*Department of Electrical and Communications Engineering, Papua New Guinea University of Technology, Lae 411, PNG*
[d,e]*Department of Electrical and Electronic Engineering, Universiti Malaysia Sarawak, Malaysia*
[f]*School of Engineering, Taylor's University, Subang Jaya, Malaysia*
[g]*Department of Computers and Technology, St. George's University, Grenada, WI*
[h]*ECE Dept., Michigan State University, East Lansing, MI, USA*

Abstract: As the aerospace industry more heavily depends on microelectronic circuits and systems for measurements and navigation, the need to ensure that their performance is not adversely affected by the intense electrostatic fields generated by electrified clouds – which are set to become more intense and heavily charged with climate change – as well as by the rapidly time changing noise signals generated by lightning strikes, both direct to the aircraft and indirect through radiated pulsed energy packets. The threat is increased with the use of non-metallic aircraft body such as composite materials. In this paper we look at the static environment of the electric cloud through a new method we have reported and in the presence of the aircraft seek to identify regions or zones where the threat to electronic circuits and control systems is greater so that when designing communication, control and microelectronic systems are placed in aircraft zones that are less electrically threatened. Moreover, the testbed we have developed, which gives opportunities for exploring the aircraft interaction beyond what is possible in a laboratory, also enabling the aircraft designer to choose the geometrical shape and materials to mitigate the electric threat to the microelectronic systems.

***Keywords*:** Safe electrical zone, micro electronic systems, wave propagation, static fields.

1. INTRODUCTION

Most aircraft are struck by lightning each year, and in the case of military aircraft, their engagement in low flying battles are severely curtailed in the highly threatening electric environment surrounding the electrified cloud, extending out to several tens of kilometers. The future land based electric vehicles as well as ships are set to heavily depend on microelectronic sensing and guiding systems for operations under all conditions of bad

weather and heavy traffic such as found close to harbors. Commercial aircraft are required to keep a distance of about 50 km from thunderclouds to avoid electric field interactions and lightning strikes, whereas for military aircraft in a battle scenario the limit can curtail its effectiveness in its movements or in battle [1].

The earlier generation of aircraft tended to use metal bodied aircraft and the instrumentation and control systems are largely mechanical or electromechanical systems that are less susceptible to the electric environment – both static and dynamic- of the thundercloud [2-5]. The advantage of composite materials is that they provide cost, weight, and safety advantages, and ease of flight control through state of the art of technologies in control, communications, and command systems. But the composite aircraft is vulnerable on issues of dissipating the electric charges and or current induced away from a non-conductive surface and the susceptibility to electromagnetic interferences (EMI) induced through indirect effects of lightning radiated electromagnetic pulses [2].

The need for computational testbeds to certify an aircraft becomes urgent since not all conditions may be replicated in laboratory tests [3-8]. In this paper, we apply a novel and innovative computational tool using 3-dimensional (3D) dipole analysis to determine the voltage, charge, and electric field induced by lightning [3] at low altitudes during ascending and or descending.

2. PRE-LIGHTNING STRIKE ELECTRIC ENVIRONMENT AROUND THE AIRCRAFT

There has been extensive research carried out by NASA to categorize and understand the electrical environment surrounding the thindercloud by either flying aircraft close to the elctrified clouds and sometimes right into them. Amongst the aircraft used is the F-16 fighter aircraft shown in Figure 1(a). The aircraft is mounted with instruments to emasure and record electric fields, magnetic fields, electric currents and voltages induced on the body of the aircraft as well as inside the electrical wiring of the aircraft connecting the communication, control, command and power system of the aircraft. In Figure 1(b) is shown the basic study reported in this paper where the aircraft is either directly under the electrified cloud (as shown in the figure) or further away. In our earlier papers (e.g. 3,4] we compared some of the resuts form our mathemtically modelled and computationally simulated resukts with available experimental results. Our method allows all kinds of aircraft to be tested and studied in a variety of position and inclination with respect to the electri charge centers inside the cloud, before the aircraft is struck by lightning, that is the static stage of the aircraft-thunderstrom interaction. The dipole electri charges are placed on the aircraft surface, and once these are determined using the technique outline in section III, we may determine the electric fields around the aircraft surface and thus electrically zone the aircraft body.

Figure 1: (a) NASA Global Hawk (Aviation Instrument Technologies Inc) Devoted to Lightning Research. (b) Dipole placements along the aircraft surface [6]

In Figure 2 is shown the zoning of an A380 with the present state of the art, largely based on laboratory tests conducted on the aircraft body, not as a whole – since a high voltage laboratory that can simulate the large thundercloud with electrodes is not available and just too huge to contemplate – but piece by piece tested in a limited size high voltage laboratory. The sound computational test bed offers huge advantage in being able to test the whole aircraft with every detail of its body included under a realistically modelled thundercloud with electric charge centres that may be situated in complex arrangements.

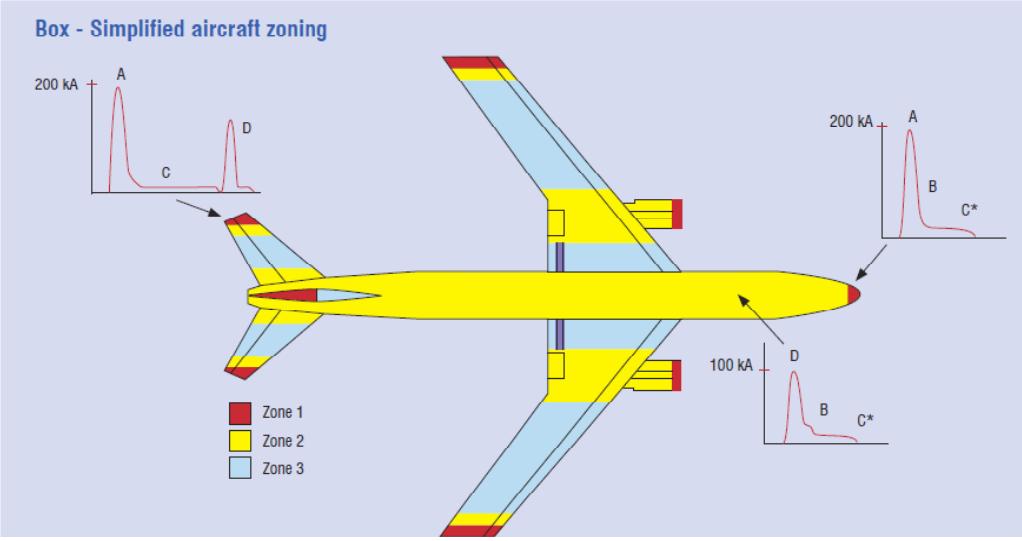

Figure 2: A possible arrangement of the aircraft zoning [5]

3. DETERMINING THE ELECTRIC CHARGES INDUCED ON THE AIRCRAFT AND THE ELECTRIC FIELDS GENRATED AROUND THE ARICRAFT BODY

The 3D dipole model is used to calculate the aircraft voltage, the charge on the surface of the aircraft, and the electric field produced by these charges using the equations given in Eq. (1) through Eq.(7). The aircraft voltage is given as

$$V_A = k \cdot q_{AD} \cdot \left(\frac{1}{r_+} - \frac{1}{r_-} \right) \tag{1}$$

where, k is a constant, q_{AD} is the aircraft dipole charge,

V_A is the aircraft voltage. r_+ and r_- are the distances from the positive and negative mono poles and their images to a selected point on the aircraft surface. In Eq. (1) V_A and q_{AD} are unknown. The only known terms in the equation are the distances from the dipole to a selected coordinate or point on the surface of the aircraft and the separation distances of the mono poles which is determined from the aircraft geometry, and the altitude of the aircraft. Thus the aircraft is at an equipotential surface. V_A is the same at all points which makes the analysis easier to handle. The cloud charge is computed from the cloud capacitance based on a given charged cloud diameter of 200 m [3]. The cloud potential is taken to be -50 MV for a negative flash. The cloud geometry is assumed to be that of a spherical Gaussian surface [4]. The charge calculation makes use of the distances between the mono poles and their mirror images on the ground at each selected point on the surface of the aircraft. Since the aircraft geometry is in 3D, three-dimensional distances (x, y, z) are used as defined in the Eq. (2). For a particular point, say p_1, on an aircraft surface, with $k = 1$ to 2 where 1 is the positive mono pole and 2 is the negative mono pole that make up the dipole, the distance from the centre of the dipole to the point p_1 on the surface of the aircraft

is given by Eq. (2). The angle between the mono poles and the point p_1 is given by Eq. (3). The same equation is also used in the calculation for the images poles, however different variables are used to denote the aircraft dipoles and their images [10].

$$\mathrm{dis}(x_{p1}, t_{p1}, z_{p1}, k) = \sqrt{(x_{p1} - x_k)^2 + (y_{p1} - y_k)^2 + (z_{p1} - z_k)^2} \tag{2}$$

$$\theta_{p1}\mathrm{dis}(x_{p1}, y_{p1}, z_{p1}) = \left[\cos^{-1}\left(\frac{(y_{p1} - y_k)}{\mathrm{dis}(x_{p1}, y_{p1}, zp_1, k)}\right)\right] \tag{3}$$

The general term for the coefficients of potential for the dipole charge is given in Eq. (4) [3].

$$q_{ADCoeff} = \left(\frac{1}{\mathrm{dis}(x_{p1}, y_{p1}, zp_1, k)}\right) - \left(\frac{1}{\mathrm{dis}(x_{p1}, y_{p1}, zp_1, k)}\right) + \left(\frac{1}{\mathrm{dis}(x_{p1}, y_{p1}, zp_1, l)}\right) - \left(\frac{1}{\mathrm{dis}(x_{p1}, y_{p1}, zp_1, l)}\right) \tag{4}$$

where, $q_{ADcoeff}$ is the coefficient of the charge due to the dipole k on the surface of the aircraft and its image l within the earth.

The voltage V_A at any point p on the aircraft surface due to n number of dipole charges is given in Eq.(5)

$$q_{ADCoeff\,1}Q_1 + q_{ADCoeff\,2}Q_2 + q_{ADCoeff\,3}Q_3 + \ldots + q_{ADCoeff\,n}Q_n = 4 \cdot \pi \cdot \varepsilon_0 \cdot V_A \tag{5}$$

From Eq.(5), the charge Q_n is defined by Eq.(6). The variable Q_n is then substituted in the equation set for voltage for the next point p_2 in order to eliminate the Q_n. The next charge variable Q_{n-1} is defined and substituted in the equation set for voltage due to the next point p_2. The procedure is repeated for $(n + 1)$ points where n is the total number of monopoles that make up the aircraft dipoles. This is simply the process of solving a set of linear equations by the substitution method. The final equation is a single equation comprising of the charge coefficients and the aircraft voltage V_A which is the only unknown term. Thus, from the computed aircraft voltage, the charges and the electric fields are determined. The electric field is computed using Eq. (7). The results are shown in Table 1 to 5 for aircraft at various altitudes and distances away from the charged cloud.

$$Q_n = \left(\frac{1}{q_{ADCoeff\,n}}\right)((4 \cdot \pi \cdot \varepsilon_0 \cdot V_A) - (q_{ADCoeff\,1}Q_1 + q_{ADCoeff\,2}Q_2 + q_{ADCoeff\,3}Q_3 + \ldots + q_{ADCoeff\,n-1}Q_{n-1}) \tag{6}$$

$$E = \frac{(k \cdot q) \cdot \bar{u}}{r^2} \tag{7}$$

Table 1
Electric charges and electric fields for Airbus A380 at an altitude of 800 m directly below charged cloud AT 1000 m altitude

Computed Voltage: –2.172 x 10^7 Volts			
Dipole Location	*Dipole Charge (C/m)*	*Electric Field (V/m)*	*Comment*
Rudder tip (D1)	4.416 x 10^{-3}	2.412 x 10^5	
Mid-right fuselage (D2)	8.674 x 10^{-6}	2.085 x 10^5	
Mid-fuselage (D3)	3.013 x 10^{-6}	1.363 x 10^5	
Mid-left fuselage (D4)	6.367 x 10^{-6}	1.287 x 10^5	

Computed Voltage: –2.172 x 10^7 Volts			
Dipole Location	*Dipole Charge (C/m)*	*Electric Field (V/m)*	*Comment*
Radome (D5)	1.999 x 10^{-4}	7.986 x 10^7	Above Breakdown E-field of 3 x 10^6 V/m
Mid-left wing (D6)	3.623 x 10^{-5}	3.514 x 10^5	
Left wing engine (D7)	6.406 x 10^{-5}	1.276 x 10^5	
Tip left wing (D8)	1.81 x 10^{-3}	1.252 x 10^7	Above Breakdown E-field of 3 x 10^6 V/m
Mid-right wing (D9)	4.875 x 10^{-5}	4.495 x 10^5	
Right wing engine (D10)	7.489 x 10^{-5}	1.288 x 10^5	
Tip right wing (D11)	1.63 x 10^{-3}	1.127 x 10^7	Above Breakdown E-field of 3 x 10^6 V/m
Left horizontal stabilizer tip (D12)	2.877 x 10^{-3}	2.873 x 10^8	Above Breakdown E-field of 3 x 10^6 V/m (becomes the entry point)
Right horizontal stabilizer tip (D13)	2.801 x 10^{-3}	2.798 x 10^8	Above Breakdown E-field of 3 x 10^6 V/m

Table 2
Electric charges and electric fields for Airbus A380 at an altitude of 500 m directly below charged cloud AT 1000 m altitude

Computed Voltage: –6.642 x 10^6 Volts			
Dipole Location	*Dipole Charge (C/m)*	*Dipole Elect. Field (V/m)*	*Comment*
Rudder (D1)	3.007 x 10^{-4}	2.501 x 10^4	
Mid-right fuselage (D2)	5.09 x 10^{-7}	2.309 x 10^4	
Mid-fuselage (D3)	1.423 x 10^{-7}	2.045 x 10^4	
Mid-left fuselage (D4)	3.751 x 10^{-7}	2.018 x 10^4	
Radome (D5)	1.31 x 10^{-5}	1.309 x 10^6	Above Breakdown E-field of 3 x 10^6 V/m
Mid-left wing (D6)	2.233 x 10^{-6}	2.838 x 10^4	
Left wing engine (D7)	3.72 x 10^{-6}	1.99 x 10^4	
Tip left wing (D8)	1.124 x 10^{-4}	7.781 x 10^5	
Mid-right wing (D9)	3.316 x 10^{-6}	3.591 x 10^4	
Right wing engine (D10)	4.335 x 10^{-6}	1.993 x 10^4	
Tip right wing (D11)	1.003 x 10^{-4}	6.941 x 10^5	
Left horizontal stabilizer tip (D12)	1.941 x 10^{-4}	1.939 x 10^7	Above Breakdown E-field of 3 x 10^6 V/m (becomes entry point)
Right horizontal stabilizer tip (D13)	1.892 x 10^{-4}	1.89 x 10^7	Above Breakdown E-field of 3 x 10^6 V/m

Table 3
Electric charges and electric fields for Airbus A380 at 800 m altitude but 1000 m away from charged cloud At 1000 m altitude

Computed Voltage: –2.821 x 10^6 Volts			
Dipole Location	*Dipole Charge (C/m)*	*Electric Field (V/m)*	*Comment*
Rudder tip (D1)	1.668 x 10^{-3}	7.566 x 10^4	
Mid-right fuselage (D2)	2.856 x 10^{-6}	6.434 x 10^4	
Mid-fuselage (D3)	2.603 x 10^{-6}	2.121 x 10^4	
Mid-left fuselage (D4)	2.769 x 10^{-6}	1.141 x 10^4	
Radome (D5)	2.178 x 10^{-5}	2.176 x 10^6	Nearing breakdown E-field of 3 x 10^6 V/m

Computed Voltage: –2.821 x 10^6 Volts			
Dipole Location	*Dipole Charge (C/m)*	*Electric Field (V/m)*	*Comment*
Mid-left wing (D6)	8.067 x 10^{-6}	7.536 x 10^4	
Left wing engine (D7)	1.818x 10^{-5}	1.611 x 10^4	
Tip left wing (D8)	4.799 x 10^{-4}	3.32 x 10^6	Above Breakdown F-field of 3 x 10^6 V/m
Mid-right wing (D9)	4.025 x 10^{-5}	3.625 x 10^5	
Right wing engine (D10)	1.652 x 10^{-5}	1.558 x 10^4	
Tip right wing (D11)	6.179 x 10^{-4}	4.274 x 10^6	Above Breakdown E-field of 3 x 10^6 V/m
Left horizontal stabilizer tip (D12)	1.155 x 10^{-3}	1.153 x 10^8	Above Breakdown E-field of 3 x 10^6 V/m (entry point)
Right horizontal stabilizer tip (D13)	1.114 x 10^{-3}	1.113 x 10^8	Above Breakdown E-field of 3 x 10^6 V/m

Table 4
Electric charges and electric fields for Airbus A380 at 800 m altitude but 5000 m away from charged cloud At 1000 m altitude

Computed Voltage: –64.308 Volts		
Dipole Location	*Dipole Charge (C)*	*Dipole Elect. Field (V/m)*
Rudder tip (D1)	1.36 x 10^{-5}	669.296
Mid-right fuselage (D2)	2.336 x 10^{-8}	586.046
Mid-fuselage (D3)	2.048 x 10^{-8}	314.979
Mid-left fuselage (D4)	2.148 x 10^{-8}	280.993
Radome (D5)	1.552 x 10^{-7}	1.551 x 10^4
Mid-left wing (D6)	6.684 x 10^{-8}	676.392
Left wing engine (D7)	1.396 x 10^{-7}	294.147
Tip left wing (D8)	3.684 x 10^{-6}	2.549 x 10^4
Mid-right wing (D9)	3.238 x 10^{-7}	2.928 x 10^3
Right wing engine (D10)	1.357 x 10^{-7}	292.391
Tip right wing (D11)	4.795 x 10^{-6}	3.317 x 10^4
Left horizontal stabilizer tip (D12)	9.401 x 10^{-6}	9.39 x 10^5
Right horizontal stabilizer tip (D13)	9.072 x 10^{-6}	9.061 x 10^5

Table 5
Electric charges and electric fields for Airbus A380 at 800 m altitude but 50000 m away from charged cloud At 1000 m altitude

Computed Voltage: –64.31 Volts		
Dipole Location	*Dipole Charge (C/m)*	*Electric Field (V/m)*
Rudder tip (D1)	1.603 x 10^{-9}	2.822
Mid-right fuselage (D2)	2.74 x 10^{-12}	2.824
Mid-fuselage (D3)	2.374 x 10^{-12}	2.826
Mid-left fuselage (D4)	2.475 x 10^{-12}	2.828
Radome (D5)	1.717 x 10^{-11}	3.309
Mid-left wing (D6)	7.927 x 10^{-12}	2.827
Left wing engine (D7)	1.601x 10^{-11}	2.827
Tip left wing (D8)	4.215 x 10^{-10}	4.059

Computed Voltage: –64.31 Volts		
Dipole Location	*Dipole Charge (C/m)*	*Electric Field (V/m)*
Mid-right wing (D9)	3.791×10^{-11}	2.846
Right wing engine (D10)	1.434×10^{-11}	2.827
Tip right wing (D11)	5.517×10^{-10}	4.748
Left stabilizer tip (D12)	1.107×10^{-9}	110.60
Right stabilizer tip (D13)	1.068×10^{-9}	106.75

4. DISCUSSION OF RESULTS OF PRE-BREAKDOWN ELECTRIC FIELDS

Tables 1 through 5 show the results for the computed voltages, charges, and electric field strength for the A380 airbus at various altitudes and distances away from the charged cloud. The results indicate that the areas with the highest electric fields exceeding the breakdown field of 3×10^6 V/m [3] have the greatest likelihood of direct attachment. These areas are the aircraft extremities, in particular the radome, the wing tips, the vertical and the horizontal stabilizers. The electric field build up at these extremities reaching or exceeding the breakdown fields can cause the ionization of the surrounding air thus initiating step leader to trigger a lightning strike It is seen that areas of high electric fields include the radome, the wing tips and the middle parts of the wings (e.g. see Table 1).

Table 1 shows the results for an A380 airbus at an altitude of 800 m, that is, at 200 m directly below the charged cloud of -50MV for a negative flash to ground. The aircraft potential computed is of -21.72 MV resulting in high charges and electric fields. The dipole electric fields calculated along the A380 aircraft show very high fields at the tip of right horizontal stabilizer reaching a peak of 2.798×10^8 V/m and the left horizontal stabilizer of 2.873×10^8 V/m. Both these fields exceeded the specified breakdown electric field of 3×10^6 V/m as defined in [3] for dry air at sea level. These two extremities with the highest electric fields are most likely to initiate bidirectional leaders towards the charged cloud centre to trigger a lightning flash connecting through the other extremities to ground. The left stabilizer is most likely to become the lightning entry point and the right to be the exit point. However, with the aircraft moving with respect to the cloud there is the possibility swept path that can develop along along the aircraft fuselage through either the radome or the tip of either wings to ground. This is shown in Figure 3 when the A380 aircraft struck by lightning at the Heathrow airport in London. These two extremities of the wings carry large electric charges and have high electric fields.

Figure 3: An A380 aircraft stuck at Heathrow airport: showing swept stroke as the aircraft moves with respect to the thundercloud (dailytelegraph.co.uk)

Table 2 shows a similar trend for an aircraft at 500 m altitude with the charged cloud at 1000 m altitude, that is, 500 m directly above the aircraft. The extremities of high electric fields are the two horizontal stabilizers and the radome. The swept path for the lightning flash is along the stabilizers and the radome. However, with the charged cloud and the aircraft moving, the capacitance, and the charges may change thus producing changes in the electric fields at the other extremities. The most likely swept path would be along the stabilizers through the fuselage and radome to ground. The stabilizer tips become the entry point while the radome becomes the lightning exit point as defined in the normative zoning standards [7].

Further, Table 3 shows the results for an aircraft at an altitude of 800 m but is at 1000 m distance away from the charged cloud. The charged cloud is at an altitude of 1000 m. The results show the charge build up initiating very large electric fields at the horizontal stabilizers and the wing tips exceeding the breakdown electric field of 3×10^6 V/m [3]. The possible entry point is most likely the left horizontal stabilizer. The swept lightning channel is along the fuselage through the wing tips to ground.

The results of Tables 4 and Table 5 show the electric fields at the aircraft extremities for the A380 airbus at an altitude of 800 m but at a distance of 5 km and 50 km away from the charged cloud, respectively. The electric fields reaches 900 kV/m for the A380 aircraft at a distance of 5 km away from the charged cloud. This field is capable of initiating a step leader when the aircraft moves close enough to the charged cloud. However, at a distance of 50 km, the electric fields are drastically reduced. This confirms the question raised in [1] on "How far is far enough?" for a safe distance of 50 km as proposed.

The results in Table 1 through Table 5 are compared with the current practice in zoning of aircraft surfaces and geometrical shapes [9]. The zones identify areas of high probability of lightning attachment depending on the electrostatic field enhancement due to electric charge build up in these areas. Moreover there are other zones to which the probability of lightning attachment being swept from an original attachment point is high. It is shown that the values in results may be used to identify and more accurately classify the zones during the aircraft design stages including protection design. The electric field enhanced regions include the rudder, the stabilizers, the radome, and the wing tips. Further, the results show a safer distance for large aircrafts such as the A380 airbus of 50 km to be safe from such a high charged cloud of -50 MV for a negative flash to ground. Fly by wire and non-metallic body aircraft designers are interested in the enhanced electric field areas of the aircraft body in order to divide the aircraft body into zones where threatening electric field enhancements and lightning strikes are highly probable and zones with minimum probability of strikes. These are the regions to be avoided when placing mission critical navigational and control systems as well as microelectronic equipment. The severe cloud-to-cloud lightning strikes in which aircraft may get engaged, is the most severe threat to navigational, microelectronic and measurement systems [10].

5. CONCLUSIONS

This paper presents a standalone, reliable tool to computationally evaluate the electric charges induced on the surface of an aircraft and the electric fields produced over the aircraft body by these electric charges. Using the knowledge of both the electric charges and the electric fields, it is possible to form zones over the aircraft body to indicate areas of high risk of lightning strike, as well areas in which microelectronic, navigation and instrumentation equipment is subjected to high electrostatic stress possibly leading the electrostatic discharges (ESD). Aircraft structure which may be classified as high risk zones include the radome, the mid-left and mid-right wing areas as well as the aircraft wing edges. It is found that even when the aircraft is flying well away from the thundercloud, some zones may still experience high electrostatic stress. The technique reported herein may also be used to study how each zone may dynamically change in experiencing electrostatic stress as the aircraft moves, or when a swept lightning stroke moves over the body of the aircraft.

Acknowledgement

The work is partly supported by the F02/FRGS/1488/2016 grant from the Ministry of Higher Education, Malaysia

REFERENCES

[1] C. Fuller, Going the Distance: Aircraft and Lightning, How far is far enough?, IEEE Int Symp on Electromagnetic Compatibility (EMC), 2016, pp. 588-593.

[2] F.L. Pitts,, B.D. Fisher, V. Mazur, R.A. Perala, Aircraft jolts from lightning bolts: electroninc systems protection, *IEEE Spectrum*, Vol. 26, Issue 7, 1988, pp. 34-38.

[3] J. Fisher, P.R.P. Hoole, K. Pirapaharan, and S.R.H. Hoole,. Applying a 3D Dipole Model for Lightning Electrodynamics of Low-Flying Aircraft. *IETE Journal of Research*, Vol.61, No.2, 2015.

[4] P.R.P. Hoole, S. Thirikumaran, H. Ramiah, J. Kanesan, and S.R.H. Hoole, Ground to Cloud Lightning Flash and Electric Fields: Interaction with aircraft and Production of Ionospheric Sprites. *Journal of Computational Engineering, Vol.2014, Article ID 869452*. http://dx.doi.org/10.1155/2014/869452., 2014.

[5] D. Morgan, C.J. Hardwick, S.J. Haigh, and A.J. Meakins, The Interaction of Lightning with Aircraft and the Challenges of Lightning Testing, *Aerospace Lab Journal. 5, ALO5-11*, pp. 1-10, 2012. http://www.aerospacelab,journal.org/sites/www.aerospacelab-journal.org/files/AL05-11, 2013.

[6] Airbus A380, Aircraft Characteristics Airport and Maintenance Planning. 2014. *Airbus Technical Data and Support and Services*.

[7] G. Sweers, B. Birch, and J. Gokcen. Lightning Strikes: Protection, Inspection, and Repair. *Boeing AERO Magazine, Issue 48, Quater 04*, pp 19-28, 2012.

[8] D. Krutilek, Z. Raida, Electromagnetic Simulation for certification of small aircraft: Direct and Indirect Effects of Lightning, 26th Int Conf. Radioelectronika, pp. 105-108, 2016.

[9] Fisher, J. P.R.P Hoole[2], K. Pirapaharan, S.R.H. Hoole, Pre-lightning Strikes and Aircraft Electrostatics , Journal of Teknologi, 2017.

[10] Fisher, J. .P.R.P Hoole, K. Pirapaharan, S.R.H. Hoole, Parameters of Cloud to Cloud and Intra-cloud Lightning Strikes to CFC and Metallic Aircraft Structures, Proc. International Symposium on Fundamentals of Engineering, IEEE Explore Digital Library, DOI: 10.1109/ISFEE.2016.7803216, pp. 1-6, Jan 2017.

[11] N. K. Haggerty, T. P. Malone and J. Crouse, "Applying High Efficiency Transformers," in IEEE Industry Applications Magazine, IEEE, November/December 1998, pp. 50-56.